THE JOURNAL OF BIOLOGICAL CHEMISTRY VOL. 285, NO. 47, pp. 36945–36957, November 19, 2010

Apolipoprotein A-I Deficiency Increases Cerebral Amyloid Angiopathy and Cognitive Deficits in APP/PS1ΔE9 Mice*[S]

Received for publication, March 26, 2010, and in revised form, August 20, 2010 Published, JBC Papers in Press, August 25, 2010, DOI 10.1074/jbc.M110.127738

Iliya Lefterov[‡1], Nicholas F. Fitz[‡2], Andrea A. Cronican[‡], Allison Fogg[‡], Preslav Lefterov[‡], Ravindra Kodali[§¶], Ronald Wetzel[§¶], and Radosveta Koldamova[‡3]

From the [‡]Department of Environmental and Occupational Health, University of Pittsburgh, Pittsburgh, Pennsylvania 15219 and the [§]Department of Structural Biology and [¶]Pittsburgh Institute for Neurodegenerative Disorders, University of Pittsburgh, Pittsburgh, Pennsylvania 15260

A hallmark of Alzheimer disease (AD) is the deposition of amyloid β (Aβ) in brain parenchyma and cerebral blood vessels, accompanied by cognitive decline. Previously, we showed that human apolipoprotein A-I (apoA-I) decreases $Aβ_{40}$ aggregation and toxicity. Here we demonstrate that apoA-I in lipidated or non-lipidated form prevents the formation of high molecular weight aggregates of $Aβ_{42}$ and decreases $Aβ_{42}$ toxicity in primary brain cells. To determine the effects of apoA-I on AD phenotype *in vivo*, we crossed APP/PS1ΔE9 to apoA-I^{KO} mice. Using a Morris water maze, we demonstrate that the deletion of mouse *Apoa-I* exacerbates memory deficits in APP/PS1ΔE9 mice. Further characterization of APP/PS1ΔE9/apoA-I^{KO} mice showed that apoA-I deficiency did not affect amyloid precursor protein processing, soluble Aβ oligomer levels, Aβ plaque load, or levels of insoluble Aβ in brain parenchyma. To examine the effect of *Apoa-I* deletion on cerebral amyloid angiopathy, we measured insoluble Aβ isolated from cerebral blood vessels. Our data show that in APP/PS1ΔE9/apoA-I^{KO} mice, insoluble $Aβ_{40}$ is increased more than 10-fold, and $Aβ_{42}$ is increased 1.5-fold. The increased levels of deposited amyloid in the vessels of cortices and hippocampi of APP/PS1ΔE9/apoA-I^{KO} mice, measured by X-34 staining, confirmed the results. Finally, we demonstrate that lipidated and non-lipidated apoA-I significantly decreased Aβ toxicity against brain vascular smooth muscle cells. We conclude that lack of apoA-I aggravates the memory deficits in APP/PS1ΔE9 mice in parallel to significantly increased cerebral amyloid angiopathy.

Alzheimer disease (AD)[4] is a late onset dementia characterized by the presence of senile plaques neurofibrillary tangles, and cognitive decline. Senile plaques are extracellular deposits of amyloid β (Aβ), a product of the proteolytic cleavage of the amyloid precursor protein (APP). The deposition of Aβ in the cerebral blood vessels, known as cerebral amyloid angiopathy (CAA), is an important pathological feature of the disease (1, 2). So far, epidemiological data suggest that AD and cardiovascular disease share common risk factors (3), such as obesity (4), high blood pressure (5, 6), high total plasma cholesterol (7), and an increased level of low density lipoproteins (8, 9). In addition, low levels of high density lipoproteins (HDL) and serum apolipoprotein A-I (apoA-I) concentrations are highly correlated with the severity of AD (10–12).

ApoA-I is the principal component of HDL with a key role in their biogenesis and function. HDL exert their primary antiatherogenic effect through reverse cholesterol transport, a process by which cholesterol is transported from peripheral organs and arterial wall foam cells to the liver and ultimately bile for excretion (13). ApoA-I and ABCA1 (ATP binding cassette transporter A1) are the key players in reverse cholesterol transport. Although the role of apoA-I in reverse cholesterol transport and the risk for cardiovascular disease is established (14), its function in the brain and role in AD are not well studied and are poorly understood.

The deposition of insoluble aggregates of Aβ into senile plaques and cognitive decline are the hallmarks of AD. Recent findings have demonstrated that memory deficits in AD mouse models precede plaque formation and display no correlation with insoluble Aβ. Instead, the accumulation of soluble oligomeric Aβ species is being considered a major pathogenic factor for the onset and progression of cognitive deficits associated with AD (15). Although the precise mechanisms are poorly understood, in general, it is believed that Aβ deposition is a result of at least three distinct processes: increased production, increased aggregation, and decreased clearance. Binding of Aβ to different proteins in the brain, including apolipoproteins (apoE, apoJ, apoA-I, and others), can affect its aggregation and deposition (16–19). ApoA-I and apoE are major lipoproteins in the brain and CSF (20, 21). Although apoE is produced mainly by astrocytes, apoA-I enters the brain from the circulation or is secreted by brain microvascular cells (22–24).

* This work was supported, in whole or in part, by National Institutes of Health, NIA, Grants AG027973 (to R. K.) and AG031956 (to I. L.). This work was also supported by Alzheimer's Association Grant IIRG-0627077 (to R. K.).

[S] The on-line version of this article (available at http://www.jbc.org) contains supplemental Figs. 1–8.

[1] To whom correspondence may be addressed: Dept. of Environmental and Occupational Health, University of Pittsburgh, BRIDG Bldg., 100 Technology Dr., Pittsburgh, PA 15219. Tel.: 412-383-6906; E-mail: iliyal@pitt.edu.

[2] Supported by NIA, National Institutes of Health, Fellowship F32.

[3] To whom correspondence may be addressed: Dept. of Environmental and Occupational Health, University of Pittsburgh, BRIDG Bldg., 100 Technology Dr., Pittsburgh, PA 15219. Tel.: 412-383-7197; E-mail: radak@pitt.edu.

[4] The abbreviations used are: AD, Alzheimer disease; Aβ, amyloid-β peptide; APP, amyloid precursor protein; CAA, cerebral amyloid angiopathy; CSF, cerebrospinal fluid; CTF, carboxyl-terminal fragment(s); MWM, Morris water maze; APP/PS1 mice, APP/PS1ΔE9 transgenic mice; WB, Western blotting; MTT, 3-(4,5-dimethylthiazol-2-yl)-2,5-diphenyltetrazolium bromide; RIPA, radioimmune precipitation assay; BisTris, 2-[bis(2-hydroxyethyl)amino]-2-(hydroxymethyl)propane-1,3-diol; ANOVA, analysis of variance; RM-ANOVA, repeated measures ANOVA; rHDL, reconstituted HDL particles; BVSMC, brain vascular smooth muscle cell(s).

The mechanisms by which apoA-I could affect AD pathogenesis are not clear. We and others have demonstrated that apoA-I binds Aβ *in vitro* and decreases Aβ-induced cytotoxicity (25–27). There is only one study published so far employing a mouse model for AD with global deletion of *Apoa-I* (28). In that study, Fagan *et al.* (28) found that the lack of apoA-I did not affect significantly insoluble Aβ levels and amyloid Aβ plaques in PDAPP/apoA-I$^{-/-}$ compared with PDAPP with wild type apoA-I. In a study with a different design, we have demonstrated that the disruption of *Abca1* in APP23 mice resulted in a significant increase of Aβ load, coinciding with the virtual absence of apoA-I in those mice and a significant decrease of apoE (29). On the other side, a chronic treatment of APP23 mice with liver X receptor ligand T0901317 (T0) increased the level of apoE and apoA-I, probably as a result of increased stability, which correlated negatively to decreased Aβ aggregation (30).

In an attempt to clarify these controversies, we have crossed APP/PS1ΔE9 mice to *Apoa-I*^{KO} mice to generate APP/PS1ΔE9/*Apoa-I*^{KO} and examined their memory deficits and amyloid pathology. Our data demonstrate that APP/PS1ΔE9/*Apoa-I*^{KO} mice have considerable memory deficits compared with mice with wild type *Apoa-I.* The impaired cognition correlated with an increased CAA. In support of these findings, our *in vitro* experiments demonstrate that apoA-I binds to Aβ and forms a complex that precludes the generation of high molecular weight oligomers and fibrils.

EXPERIMENTAL PROCEDURES

Materials

Human apolipoprotein A-I and reconstituted HDL were from Meridian Life Science Inc. (Saco, ME); Aβ_{40} and Aβ_{42} were synthesized at Keck's facility (Yale University); the Amplex Red cholesterol assay kit was from Invitrogen. Avertin and Hoechst 33342 were from Sigma; and the protease inhibitor mixture was from Calbiochem. The enhanced chemiluminescence detection kit was from GE Healthcare. The 3-(4,5-dimethylthiazol-2-yl)-2,5-diphenyltetrazolium bromide (MTT) assay kit, was from Trevigen (Gaithersburg, MD), and the Caspase-Glo 3/7 assay was from Promega (Madison, WI). All other reagents and materials for cell culture and general use (if not specified) were from Invitrogen and Fisher, respectively.

Mice

The study fully conformed to the guidelines outlined in the Guide for the Care and Use of Laboratory Animals from the United States Department of Health and Human Services and was approved by the University of Pittsburgh Institutional Animal Care and Use Committee. APP/PS1ΔE9 (B6.Cg-Tg(APPswe, PSEN1ΔE9)85Dbo/J) transgenic mice and mice with targeted disruption of mouse *Apoa-I* (B6.129P2-*Apoa- I*$^{tm1Unc/J}$), both strains on C57BL/6J background, were purchased from Jackson Laboratory (Bar Harbor, ME). APP/PS1ΔE9, express mutant familial variants of human APP with Swedish mutation (APPsw), and human PS1 (presenilin 1) with deletion in exon 9 (PS1ΔE9). APP/PS1ΔE9 mice (referred to as APP/PS1) were cross-bred to *Apoa-I*^{KO} to generate APP/PS1ΔE9/*Apoa-I*^{KO} (referred to as APP/PS1/KO). APP/PS1ΔE9 mice with wild type mouse *Apoa-I* (referred to as APP/PS1/WT) were used as controls. In addition, for behavioral tests, we used non-transgenic wild type (WT/WT) and *Apoa-I*^{KO} mice (WT/KO). All mice were littermates and were fed normal mouse chow. *Abca1*^{KO} and *Apoe*^{KO} mice were used as controls for WB.

Morris Water Maze

Behavioral tests to assess spatial navigational learning and memory retention were performed with a modified version of the Morris water maze (MWM) as before (31, 32) with minor modifications. Briefly, in a circular pool of water (diameter 122 cm, height 51 cm, temperature 21 ± 1 °C), we measured the ability of mice to form a representation of the spatial relationship between a safe but invisible (submerged 1 cm below the water level) platform (10 cm in diameter) and visual cues surrounding the pool of water. The platform was located in the center of one of the four quadrants of the pool (*e.g.* the target quadrant). Several extra maze cues were distributed across the walls surrounding the pool. Animals received a habituation trial, during which the animals were handled for several min by the experimenter and allowed to explore the pool of water without the platform present. Beginning the next day, they received four daily hidden platform training (acquisition) trials with 10–12-min intertrial intervals for five consecutive days. Animals were allowed 60 s to locate the platform and 20 s to rest on it. Mice that failed to find the platform were lead to the platform by the experimenter and allowed to rest there for 20 s. Acquisition training was performed for 5 consecutive days. Twenty-four hours following the last acquisition trial, a single 60-s probe trial was administered to assess spatial memory retention. For the probe trial, animals were returned to the maze as during training but with no platform present. Two hours after the probe trial, the visual cue test was performed with the escape platform lifted 1 cm above water level and shifted to the target quadrant. A flag was added to the target platform as a visual cue. This is used to evaluate the visual perception of the mice. Mice exhibiting difficulty in finding the visible platform were excluded from the final analysis. In addition, the swimming speed during the acquisition phase was analyzed (this was used to evaluate the locomotor activity), and mice with swimming speed significantly lower than the mean speed were disqualified from the analysis. Performance was recorded with an automated tracking system (AnyMaze, Stoelting Co.) during all acquisition and probe trials. During the acquisition trials, acquisition time (latency to reach the platform) and path length (distance swum to the platform) were subsequently used to analyze and compare the performance between different treatment groups. The relative time spent in each of the four quadrants and the number of crossings of the former platform location were recorded and analyzed during the probe trials.

Animal Tissue Processing

Mice were anesthetized by intraperitoneal injection of Avertin (Sigma) 250 mg/kg body weight) and perfused transcardially with 25 ml of cold 0.1 M PBS (pH 7.4). Brains were rapidly removed and divided into hemispheres, and in one of the hemispheres, the cortex and hippocampus were separated from the olfactory bulbs, subcortical structures, and cerebellum. These

brain structures were snap-frozen on dry ice; the other hemisphere was drop-fixed in 4% phosphate-buffered paraformaldehyde at 4 °C for 48 h before storage in 30% sucrose.

Histology and Immunohistochemistry

All procedures were as reported previously (31) with the following modifications: Histoprep (Fisher)-embedded hemibrains were cut in the coronal plane at 30-μm sections and stored in a glycol-based cryoprotectant at −20 °C until staining. Sections were selected 300 μm apart, starting from a randomly chosen section ~150 μm caudal to the first appearance of the CA3 and dentate gyrus. X-34 (1,4-bis(3-carboxy-4- hydroxyphenylethenyl)-benzene) is a highly fluorescent derivative of Congo Red that can be used to detect senile plaques and was provided by W. Klunk (University of Pittsburgh). X-34 staining and immunoreactivity against glial fibrillary acidic protein were performed on mounted sections as described previously (31).

Western Blotting, ELISA, and Dot Blotting

The frozen hemibrains (only cortices and hippocampi) were homogenized in tissue homogenization buffer (250 mM sucrose, 20 mM Tris base, 1 mM EDTA, 1 mM EGTA, 1 ml/100 mg of tissue), and protease inhibitors (10 μg/ml leupeptin, 10 μg/ml apportion, and 10 μg/ml 4-(2-aminoethyl)-benzenesulfonyl fluoride) as before (29, 33). After homogenizing with tissue homogenizing buffer, the brains were additionally extracted with RIPA buffer, TBS, or formic acid. The term "soluble Aβ" refers to non-plaque-associated Aβ, extracted by TBS or RIPA buffer. The term "insoluble" defines plaque-associated Aβ extracted with formic acid. Aβ ELISA and WB were performed essentially as described previously (31).

Detection of APPfl—To detect APPfl, carboxyl-terminal fragments CTFα and CTFβ (the result of α- and β-secretase cleavages), soluble Aβ, and *Abca1* protein extracts were prepared from the initial homogenate using 2× RIPA buffer. APPfl and CTFα/β were detected by SDS-PAGE followed by WB as before (34) using the C8 carboxyl-terminal antibody (provided by Matthias Staufenbiel, Novartis).

Detection of Soluble Aβ—To detect soluble Aβ by WB, proteins extracted with RIPA buffer were resolved on 4–12% BisTris gels, followed by WB with 6E10 antibody. *Abca1* was detected using monoclonal antibody ab7360 (Abcam, Cambridge, MA) on 8% Tris-glycine gels.

Detection of ApoE and ApoA-I—To detect apoE and apoA-I, the initial homogenate was spun at 100,000 × *g*, and supernatant was used for SDS-PAGE followed by WB. ApoE was detected on WB using M-20 polyclonal antibody (Santa Cruz Biotechnology, Inc., Santa Cruz, CA) and apoA-I using a mouse-specific rabbit polyclonal antibody (Rockland, Gilbertsville, PA). β-Actin was used as a loading control for all WB and was detected by monoclonal antibody from Santa Cruz Biotechnology, Inc.

Soluble and Insoluble Aβ Measurements—For soluble and insoluble Aβ measurements, we used a sequential extraction procedure. Soluble proteins were extracted from the initial homogenate using a Dounce homogenizer and centrifugation at 100,000 × *g* for 1 h at 4 °C. Supernatant was saved and used to detect soluble Aβ and soluble oligomers. Insoluble Aβ was extracted from the remaining pellet using formic acid as before (29, 33). Soluble and insoluble Aβ_{40} and Aβ_{42} level were determined in each of these extracts by ELISA. ELISA for Aβ was performed using 6E10 (Covance, Pittsburgh, PA) as a capture antibody; anti-Aβ_{40} (G2-10 mAb) and anti-Aβ_{42} (G2-13 mAb) monoclonal antibodies conjugated to horseradish peroxidase (Genetics Co., Schlieren, Switzerland) were used as the detection antibodies. The final values of Aβ were based on Aβ_{40} and Aβ_{42} peptide standards, and normalized amounts of Aβ were expressed as pmol/mg.

Soluble Aβ Oligomers—Soluble Aβ oligomers were detected in the soluble brain extract (as described above) (31, 35, 36). For the detection of prefibrillar Aβ oligomers, 1 μg of protein was spotted on a nitrocellulose membrane and probed with A11 antibody (1:2,000). Fibrillar Aβ oligomers were detected on similarly performed dot blotting by spotting 1 μg of protein and using OC antibody (1:10,000). A11 and OC antioligomeric antibodies were generously provided by Suhail Rasool, Jessica Wu, and Charles Glabe (University of California, Irvine, CA). The membranes were probed with anti-rabbit secondary antibody, and the immunoreactive signals were visualized using enhanced chemiluminescence and quantified densitometrically. The exact same amount of samples was spotted on additional dot blots and probed with 6E10 and Bradford reagent for normalization.

Methods for Evaluation of CAA

Extraction of Insoluble Aβ from Blood Vessels—Isolation of blood vessels from cortices and hippocampi was done as previously reported (37) with slight modification. Briefly, 1.5 ml from the initial brain homogenate (tissue homogenizing buffer; see above) was washed with and then resuspended by pipetting in 1.5 ml of blood vessel isolation buffer (0.1 M NH_4CO_3, 5 mM EDTA, 0.01% sodium azide, and protease inhibitor mixture). Homogenates were centrifuged (100,000 × *g*, 1 h, 4 °C), and pellets were resuspended in 500 μl of 0.1 M NH_4CO_3 plus 7% SDS (plus protease inhibitor mixture) and stirred for 4 h. Tissues were then filtered through 70- and 40-μm mesh filters to isolate blood vessels from cortical and hippocampal filtrate. Isolated blood vessels were washed and centrifuged (6,000 × *g*, 10 min, 4 °C) to remove supernatant, pellet was resuspended in 70% formic acid, and insoluble Aβ was extracted as before (29). ELISA for insoluble Aβ_{40} and Aβ_{42} was performed as above for total brain Aβ.

Morphological Quantification of CAA—For morphological quantification of CAA, we used a protocol published by Wilcock *et al.* (38) with minor modification. Briefly, the same five sections 300 μm apart stained with X-34 (as used for parenchymal Aβ load; see above) were reanalyzed. Microscopic examination was carried out using a Nikon Eclipse 80i microscope, and images were captured by a Nikon DS Qi1MC camera at an overall magnification of 100×. In a double blind manner, CAA was quantified based on morphological criteria. The area occupied by CAA was determined by examining the entire area of each section using Metamorph 7.0 (Molecular Devices, Sunnyvale, CA). For confocal microscopy, sections were first stained with CY3-labeled smooth muscle actin antibody (Invitrogen) to stain the smooth muscle found in vessel walls and then with

X-34. Confocal microscopy was performed on an Olympus Fluoview 1000 inverted confocal microscope.

Cholesterol Analysis

Cholesterol in the brain was measured as before (39) with slight modification. Brain samples were prepared for cholesterol analysis by sonication in tissue homogenizing buffer (see above), diluted 5-fold in 20 mM Tris buffer, and then subjected to enzymatic analysis for total cholesterol using the Amplex Red cholesterol kit (Sigma). The values were normalized to the total protein concentration in the samples.

Aβ Aggregation and Assays for Monitoring Aggregation

Stock solutions of synthetic $A\beta_{42}$ were disaggregated according to the method described previously by O'Nuallain *et al.* (40). In brief, the method involves two steps: 1) the dissolution and breakdown of aggregated structures through sequential steps of treatment with trifluoroacetic acid (TFA) and hexafluoro-2-propanol, followed by removal of the solvents, and 2) aqueous dissolution of the resulting disaggregated peptide film, followed by high speed centrifugation (100,000 × *g*) for 1 h to remove trace aggregates. This method generates monomeric $A\beta_{42}$ in a concentration between 10 and 25 μM. Aβ aggregation reactions were performed in PBS with 0.05% NaN_3 at 37 °C without shaking. To determine the effect of human or mouse apoA-I, 3 μM Aβ was incubated with different concentrations of apoA-I, and aggregation was monitored by thioflavine T fluorescence or WB. As a source of mouse apoA-I, we used a recombinant mouse apoA-I generously provided by Dr. M. Phillips (Children's Hospital of Philadelphia, Philadelphia, PA).

Thioflavine T Assays—Thioflavine T assays were performed as before (25).

SDS-PAGE—For SDS-PAGE, Aβ complexes were resolved on 4–12% BisTris NUPAGE gels, followed by WB with 6E10 antibody. Human apoA-I was detected on the same gels using anti-human monoclonal antibody (Calbiochem) or mouse-specific anti-mouse apoA-I antibodies (see above).

Electron Microscopy—For Electron microscopy, 5 μl of sample was placed on a freshly glow-discharged carbon-coated grid, adsorbed for 2 min, and excess solution was blotted using filter paper. The grid was washed with deionized water before staining with 5 μl of freshly filtered uranyl acetate solution (1%, w/v) for 15 s. Excess stain was blotted, and the grid was allowed to air-dry. Grids were imaged on a Tecnai T12 microscope (FEI, Hillsboro, OR) operating at 120 kV and ×30,000 magnification and equipped with an UltraScan 1000 CCD camera (Gatan, Warrendale, PA) with postcolumn magnification of 1.4×.

Cell Culture, Cytotoxicity, and Apoptosis Assays

Primary Neuronal Cultures—Primary neuronal cultures were generated from dissociated cortices and hippocampi of 17–19-day-old Sprague-Dawley rat embryos, and neurons were plated at a density of 1×10^5/ml in 24-well plates on cover slides as described previously (34). Neurons were treated with fibrillar $A\beta_{42}$ with or without human apoA-I at *in vitro* day 5. Fibrillar Aβ was generated by incubating 250 μM $A\beta_{42}$ with or without 25 μM human apoA-I for 72 h at 37 °C. Controls received vehicle instead of apoA-I. After the incubation, $A\beta_{42}$ (with or without human apoA-I) preparations were additionally diluted to a final concentration of 25 μM for Aβ and 2.5 μM for apoA-I in culture medium, and neurons were treated for 48 h.

Hoechst 33342 Staining—Prior to staining, the cells were fixed with 4% paraformaldehyde for 30 min at room temperature. Hoechst solution was added to the fixed cells for 30 min, and they were examined by fluorescence microscopy, as before (41). Apoptotic cells were identified by condensation and fragmentation of nuclei. To evaluate the percentage of apoptotic cells, we counted three independent microscopic fields for each slide. Each experiment was performed in triplicate, and the percentage of apoptotic cells was calculated as the ratio of apoptotic cells to total cells counted times 100. A minimum of 400 cells was counted for each treatment. Under control conditions, 4–8% of neuronal cells exhibited apoptotic morphology at *in vitro* day 5.

Human Brain Vascular Smooth Muscle Cells—Human brain vascular smooth muscle cells (Sciencell Research Laboratories, Carlsbad, CA) were plated at a density of 1×10^4 cells/well in a flat bottom 96-well plate with 100 μl of smooth muscle cell medium provided by the same company. Cells were treated in DMEM/F-12 with 2% delipidated serum. Apoptosis was evaluated by a Caspase-Glo 3/7 assay performed according to the manufacturer's instructions. Briefly, the caspase assay was added 1:1 to cells after treatment and then transferred to a 96-well optical bottom white side plate (Fisher).

Cytotoxic Effects of $A\beta_{42}$—The cytotoxic effects of $A\beta_{42}$ were assessed also by MTT reduction with rat pheochromocytoma PC12 cells as described previously (25). Briefly, exponentially growing PC12 cells (20,000 cells/well) were plated with fresh culture medium (100 ml) on 96-well tissue culture plates and treated 24 h after plating. Aβ cytotoxicity was quantitatively assessed by the MTT assay kit, as described previously (25).

Statistical Analysis

All results are reported as means ± S.E. Statistical significance of differences between mean scores during the acquisition phase of training in the MWM was assessed by two-way repeated measures ANOVA (general linear model/RM-ANOVA) and a Tukey *post hoc* test for multiple comparisons using genotype and trial block number as sources of variation and mouse gender as a covariate. In addition, to determine the differences between genotypes for each trial day, we used one-way ANOVA with a Tukey *post hoc* test. To evaluate the differences in the parameters during the probe trial, we used one-way ANOVA with a Tukey *post hoc* test. Comparisons of percentage immunoreactivity, X-34 staining, and total cholesterol levels between treatments were performed using Student's *t* test. All statistical analyses were performed in GraphPad Prism, version 4.0 (La Jolla, CA) or SPSS, version 16, release 2009 (Chicago, IL), and differences were considered significant where p was <0.05.

RESULTS

Human ApoA-I Decreases $A\beta_{42}$ Aggregation and $A\beta_{42}$-induced Cell Death—Previously, we demonstrated that human apoA-I decreases $A\beta_{40}$ aggregation and toxicity in primary neurons (25). To examine the effect of apoA-I on $A\beta_{42}$ aggregation, $A\beta_{42}$ was incubated with equimolar concentrations of lipid-

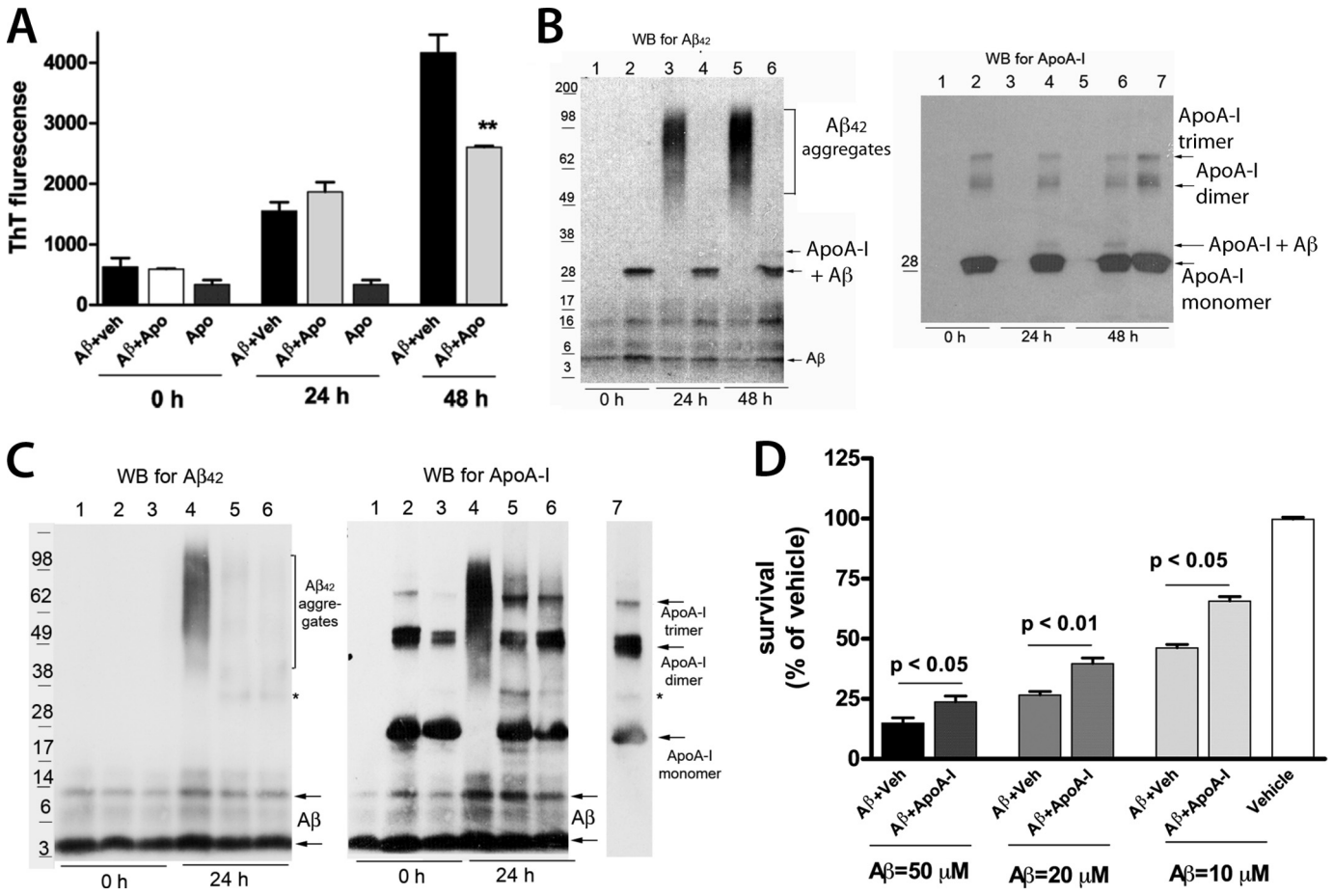

FIGURE 1. **Human apoA-I decreases Aβ aggregation and Aβ_{42}-induced Cell Death.** 3 μM Aβ_{42} was incubated with equimolar concentration of lipid-free human apoA-I as described under "Results," and Aβ_{42} aggregation was examined by thioflavine T fluorescence and WB for Aβ or apoA-I. *A*, thioflavine fluorescence demonstrates that human apoA-I decreases Aβ_{42} aggregation 48 h after the start of the incubation. **, $p < 0.01$ compared with Aβ + vehicle (*Aβ + Veh*) at 48 h by a two-tailed *t* test. *B*, aliquots of the samples shown in *A* were resolved on SDS-PAGE followed by WB for Aβ_{42} (*left*) and human apoA-I (*right*). *Lanes 1*, *3*, and *5*, Aβ_{42} plus vehicle; *lanes 2*, *4*, and *6*, Aβ plus human apoA-I. *Lane 7*, apoA-I alone. ApoA-I alone does not interact with 6E10 antibody (not shown). On the *left side* of each blot we show the migration of the protein standards, and on the *right*, *arrows* point to Aβ and apoA-I. Note the arrows pointing to the band representing the SDS-stable complex between Aβ and human apoA-I (*Aβ + ApoA-I*), which is missing in the *lanes* with Aβ plus vehicle. *C*, lipidated human apoA-I inhibits Aβ_{42} aggregation similarly to lipid-free human apoA-I. 3 μM Aβ_{42} was incubated with reconstituted high density lipoproteins (*rHDL*) containing human apoA-I as the only protein. After 24 h, aliquots of the samples were resolved on SDS-PAGE followed by WB for Aβ_{42} (*left*) and apoA-I (*right*). The molar concentration of rHDL was calculated according to human apoA-I concentration. *Lanes 1* and *4*, Aβ_{42} plus vehicle. In *lanes 2* and *5*, the Aβ_{42}/apoA-I-ratio is 1:1; in *lanes 3* and *6*, the ratio is 2:1. Following WB for Aβ_{42}, the membranes without stripping were probed with anti-human apoA-I antibody. The *arrows* point to apoA-I monomers, dimmers, and trimers, and an *asterisk* marks a nonspecific band. *D*, Aβ_{42} increases cell death in a concentration-dependent manner, and human apoA-I protects against it. Primary neurons were incubated for 24 h with increasing concentrations of Aβ_{42} with or without apoA-I used in equimolar concentrations, and survival was examined by an MTT assay. The data are results of two experiments in triplicate. Analysis was by Student's *t* test. *Error bars*, S.E.

free human apoA-I for different periods of time. The aggregation was monitored by a thioflavine T fluorescence assay and SDS-PAGE followed by WB. As shown in Fig. 1*A*, human apoA-I decreased Aβ aggregation 48 h after the start of incubation. WB for Aβ (Fig. 1*B*) demonstrates that when Aβ_{42} is incubated with vehicle, there is a formation of high molecular weight aggregates (above 60 kDa) that are missing if Aβ_{42} is incubated with apoA-I (Fig. 1*B*). Moreover, as shown before for Aβ_{40} (25), human apoA-I formed SDS-stable complexes with Aβ_{42} (Fig. 1*B*, *arrows* on the *left*). For comparison, in supplemental Fig. 1*A*, we show that human apoA-I similarly inhibits Aβ_{40} aggregation. Also, as visible in the figure, the molecular weight of Aβ_{40} aggregates was lower compared with the molecular weight of Aβ_{42} aggregates.

To examine if the lipidated apoA-I has the same effect as lipid-free apoA-I on the aggregation of Aβ_{42}, we used reconstituted HDL particles (rHDL) that contain human apoA-I as the only apolipoprotein. Aβ_{42} was incubated with rHDL, and aggregation was examined by WB 24 h later. Fig. 1*C* shows that Aβ aggregation was reduced significantly when lipidated human apoA-I was used in two different concentrations (in *lane 5*, the apoA-I/Aβ_{42} molar ratio is 1:1, and in *lane 6*, the ratio is 1:2). We also noticed that in contrast to lipid-free apoA-I, in this experiment, we did not detect a formation of SDS-stable complex between Aβ_{42} and lipidated apoA-I. These results demonstrate that lipidated human apoA-I inhibits Aβ_{42} aggregation similarly to non-lipidated human apoA-I.

To determine the inhibitory effect of apoA-I on Aβ-induced toxicity, primary neurons were treated with increasing concentrations of Aβ_{42} with or without human apoA-I, and cell survival was examined by an MTT assay. Fig. 1*D* shows that incubation of neurons with Aβ decreased neuronal survival in a

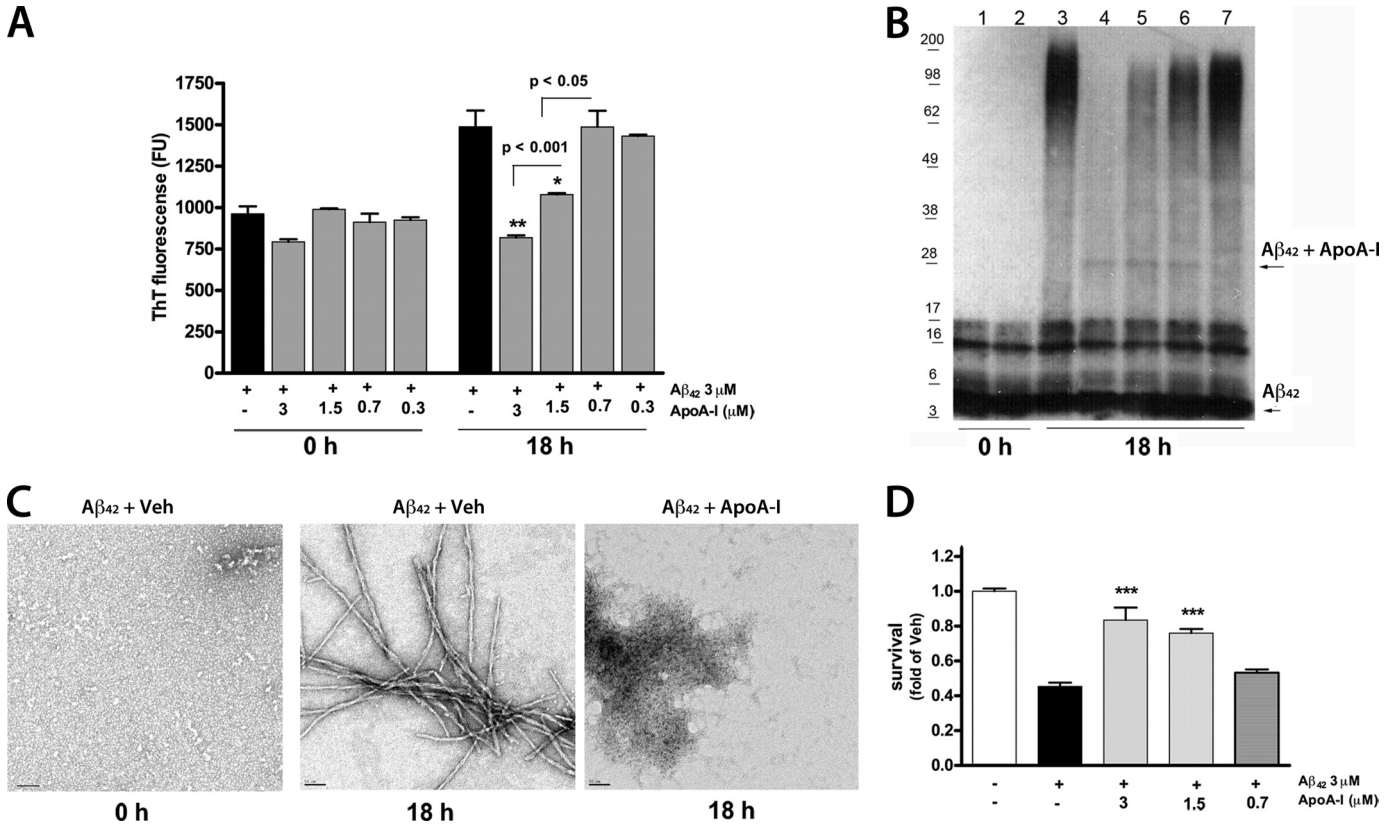

FIGURE 2. **Mouse apoA-I decreases Aβ_{42} aggregation and Aβ_{42}-induced cell death.** Aβ_{42} (3 μM) was incubated with decreasing concentrations of mouse apoA-I for 18 h, as described under "Experimental Procedures," and Aβ aggregation and cell death were examined. *A*, thioflavine fluorescence demonstrates that mouse apoA-I decreases Aβ_{42} aggregation in a concentration-dependent manner. Pairwise comparisons by *t* test are shown. **, $p < 0.01$; *, $p < 0.05$ *versus* Aβ alone. *B*, aliquots of the samples were resolved on SDS-PAGE followed by WB for Aβ. *Lanes 1* and *3*, Aβ plus vehicle; *lanes 2* and *4*, Aβ plus 3 μM apoA-I; *lane 5*, Aβ plus 1.5 μM apoA-I; *lane 5*, Aβ plus 0.75 μM apoA-I; *lane 6*, Aβ plus 0.3 μM apoA-I. The *arrows* point to Aβ and a *faint band* representing the Aβ-apoA-I complex. *C*, aliquots of 3 μM Aβ_{42} with or without 3 μM mouse apoA-I (as shown in *B*) were analyzed by transmission electron microscopy. Shown are electron micrographs of Aβ_{42} plus vehicle (*Veh*) at the start of incubation (*0 h*) and 18 h later (*18 h*); Aβ_{42} plus mouse apoA-I is shown 18 h after the start of incubation. *Scale bars*, 50 nm. *D*, PC12 cells were treated for 48 h with Aβ_{42} with or without mouse apoA-I (prepared as in *A* at time 0), and cell survival was determined by an MTT assay. ***, $p < 0.001$ *versus* Aβ plus vehicle by Student's *t* test. *Error bars*, S.E.

concentration-dependent manner, and the addition of human apoA-I increased it. To confirm the protective effect of human apoA-I against Aβ-induced neuronal death, we used Hoechst staining of apoptotic nuclei. Prior to treatment, Aβ_{42} was preincubated with human apoA-I (Aβ/apoA-I molar ratio 10:1) or vehicle. Then the preparations were used to treat primary mouse neurons. As visible in supplemental Fig. 2, preincubation of Aβ_{42} with apoA-I significantly decreased apoptotic cell death caused by Aβ_{42}. Altogether, the results from these experiments clearly demonstrate that human apoA-I decreases Aβ_{42} aggregation and Aβ_{42}-induced cell death.

Mouse ApoA-I Decreases Aβ_{42} Aggregation and Aβ_{42}-induced Cell Death—To examine if mouse apoA-I has a similar effect on Aβ_{42} aggregation and toxicity, we used recombinant mouse apoA-I (42) and performed similar experiments as with human apoA-I. Fig. 2*A* shows that the inhibition of Aβ_{42} aggregation is concentration- dependent, as measured by a thioflavine T assay. This result was confirmed by SDS-PAGE with a dose-dependent decrease of high molecular weight Aβ_{42} aggregates, visible on the WB (Fig. 2*B*). We also observed Aβ-apoA-I SDS-stable complex, but its level did not correlate with the level of the inhibition of Aβ aggregation, suggesting that this complex is irrelevant to the process of aggregation. To determine more precisely the structure of Aβ aggregates, aliquots of the samples shown in Fig. 2C were examined by electron microscopy. Fig. 2*C* shows that 18 h after the start of the incubation, Aβ_{42} plus vehicle formed mature fibrils, and the addition of mouse apoA-I to Aβ_{42} completely inhibited the formation of fibrils. Instead, Aβ formed amorphous unstructured material. From these experiments, we conclude that mouse apoA-I inhibits Aβ_{42} aggregation probably by increasing its conversion into benign protein assemblies, as reported before for other molecules (43). Finally, we determined that mouse apoA-I inhibits the toxic effects of Aβ in PC12 cells (Fig. 2*D*). Altogether, the results of these experiments led to the conclusion that mouse apoA-I inhibits Aβ aggregation, which correlates to a decreased Aβ_{42} toxicity.

Deficiency of ApoA-I Exacerbates Cognitive Deficits in APP/PS1/KO Mice—Our next goal was to determine if the effects of mouse apoA-I on Aβ observed *in vitro* translate in changes of the phenotype in experimental AD model mice. To this end, we used mice expressing mutated human APP and PS1 genes (APP/PS1) crossed to *ApoA-I*^{KO} mice with targeted disruption of mouse *Apoa-I*, and generated APP/PS1/KO mice. These mice were compared with age- and gender-matched APP-expressing mice with intact mouse *Apoa-I* (APP/PS1/WT). To examine how mouse apoA-I deficiency affects cognitive performance, 12-month-old APP/PS1/KO and APP/PS1/WT

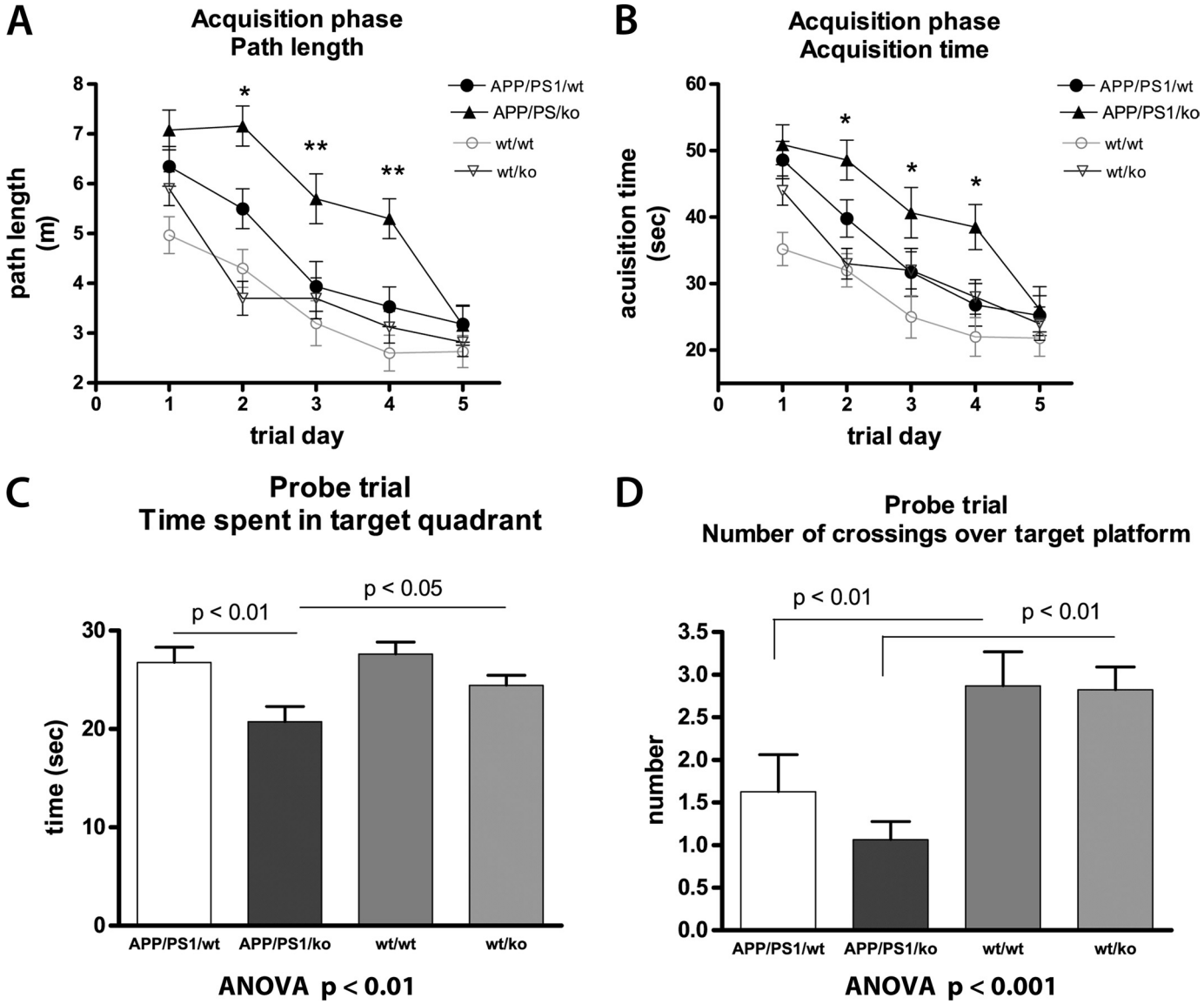

FIGURE 3. **The deletion of mouse apoA-I aggravates cognitive deficits in APP/PS1 mice.** Twelve-month-old APP/PS1/WT and APP/PS1/KO mice were tested for memory deficits using the MWM paradigm. Non-transgenic WT/WT and WT/apoA-I^{KO} mice (WT/KO) were used as controls. *A* and *B* show the acquisition phase of MWM. *A*, path length. Analysis by RM-ANOVA demonstrates a significant genotype effect on path length ($F_{(3,81)} = 12.4$, $p < 0.001$). Analysis by one-way ANOVA demonstrates statistical significance between APP/PS/WT and APP/PS/KO for trial days 2, 3, and 4. *B*, escape latency. Analysis by RM-ANOVA shows a significant genotype effect on escape latency ($F_{(3,81)} = 6.71$, $p < 0.001$). Analysis by one-way ANOVA demonstrates statistical significance between APP/PS1/WT and APP/PS1/KO for trial days 2, 3, and 4. In *A* and *B*, mouse gender had no effect on the performance when gender was used as a covariate in RM-ANOVA analysis, $p = 0.52$. *C* and *D*, probe trial. *C*, time spent in the target quadrant. *D*, number of crossings over the previous location of the platform. *C* and *D*, analysis by one-way ANOVA, followed by Tukey's post-test. For APP/PS1/WT, $n = 11$ males and 7 females; APP/PS1/KO, $n = 10$ males and 6 females; WT/WT, $n = 14$ males and 10 females; WT/KO, $n = 10$ males and 8 females. *Error bars*, S.E.

mice were tested in MWM, assessing their spatial learning and memory retention. Age- and gender-matched non-transgenic wild type (WT/WT) and *Apoa-I*^{KO} (WT/KO) mice were used as controls. As illustrated in Fig. 3, *A* and *B*, during the acquisition phase, all mice improved their performance with daily training, exemplified by their path length (Fig. 3*A*) and acquisition time (Fig. 3*B*). As seen in Fig. 3, *A* and *B*, APP/PS1/WT and APP/PS1/KO mice differed significantly from their respective wild type controls. The deletion of *Apoa-I* did not affect the cognitive performance in the non-transgenic mice (WT/WT *versus* WT/KO; no significant difference in path length and acquisition time). In contrast, the lack of mouse apoA-I significantly worsened the acquisition of spatial memory in the APP/PS1 transgenic mice. As demonstrated in Fig. 3, *A* and *B*, during the training phase, APP/PS1/KO mice learned the task significantly more slowly than APP/PS1/WT animals, specifically on the second, third, and fourth trial days (Fig. 3, *A* and *B*). The results presented in Fig. 3, *C* and *D*, demonstrate that the cognitive deficits in APP/PS1/KO mice persisted during the probe trial of MWM, which assesses memory retention; APP/PS1/KO performed significantly worse than their non-transgenic controls (Fig. 3, *C* and *D*). Most importantly, APP/PS1/KO spent significantly less time than APP/PS1/WT mice in the quadrant where the platform was previously located (Fig. 3*C*, $p < 0.01$), suggesting impaired ability to form spatial memory. The diminished memory performance in APP/PS1/KO mice was not a

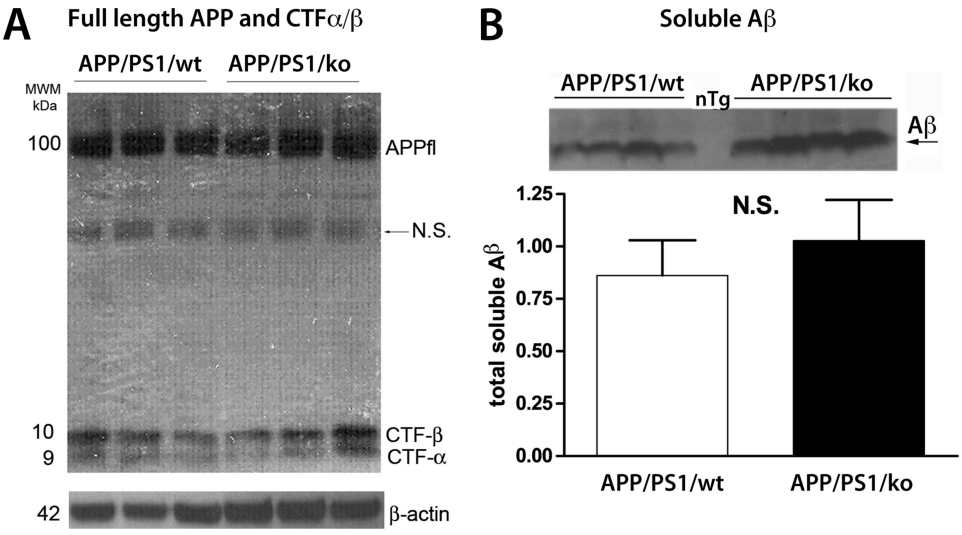

FIGURE 4. **The deletion of apoA-I does not affect APP processing and soluble Aβ level.** *A* and *B*, soluble proteins were extracted from the cortices and hippocampi of APP/PS1/WT and APP/PS1/KO mice using RIPA buffer as described under "Experimental Procedures." *A*, WB for full-length APP (APPfl) and carboxyl-terminal fragments generated by β-and α-secretases cleavages (CTFα/β). APPfl and CTFα/β were normalized on β-actin and quantified but did not show a difference between the genotypes (not shown). *B*, WB for total soluble Aβ was performed on 4–12% NU PAGE gels, followed by WB with 6E10 antibody. For quantification, Aβ intensity was normalized on β-actin shown in *A*. For *A* and *B*, shown are representative pictures from 10–14 mice/group. *N.S.*, not significant. *Error bars*, S.E.

result of impaired locomotor activity, because there was no significant difference in the swimming speed between APP/PS1/WT and APP/PS1/KO mice (0.134 *versus* 0.138 m/s). There was no difference in the visual cue test either (not shown), suggesting that mice did not have visual problems. Collectively, the results from the MWM test demonstrate that the deletion of mouse apoA-I significantly worsens memory deficits in transgenic mice expressing human APP and PS1 genes but not in wild type mice.

Lack of ApoA-I Does Not Affect APP Processing and Soluble Aβ in APP/PS1 Mice—The results from the MWM test suggested that the observed memory deficits in 12-month-old APP/PS1/KO mice could be related to the expression of mutated human APP and PS1 or to the level of amyloid deposition in their brains. Therefore, we first compared APP processing in APP/PS1/KO and APP/PS1/WT mice. As shown in Fig. 4, lack of apoA-I changed neither the level of full-length APP nor its processing; Fig. 4*A* demonstrates that there was no difference in the levels of CTFα/β. In addition, we also examined the secreted soluble fragment products of α- and β-secretases cleavages, namely sAPPα and sAPPβ, but did not find a difference between APP/PS1/KO and wild type (APP/PS1/WT) mice (not shown). To examine the level of soluble Aβ in the same extract, we used WB with 6E10 antibody with an epitope at amino acids 1–16 of Aβ peptide. The antibody detects total Aβ peptides with 40, 42, or 43 amino acids or shorter lengths. As shown in Fig. 4*B*, lack of apoA-I did not affect the secretion of the total soluble Aβ. WB for Aβ from all mice is shown in supplemental Fig. 3. Our conclusion is that the deletion of *Apoa-I* in APP/PS1 mice does not affect APP processing and soluble Aβ level.

The Deletion of Apoa-I Does Not Affect Protein Levels of Abca1 and apoE and Cholesterol Concentration in APP/PS1/KO Mice—ApoA-I is the major apolipoprotein of HDL in the periphery and of HDL-like particles in the brain. Because it is possible that the deletion of *Apoa-I* could lead to a compensatory increase of other proteins that participate in the generation of HDL, apoE and Abca1 in particular, we examined their protein levels by WB. As shown in Fig. 5, *A–C*, the deletion of *Apoa-I* did not affect Abca1 and apoE protein levels and cholesterol concentration in APP/PS1/KO mice. There was no difference in apoE and Abca1 protein levels in non-transgenic mice either (supplemental Fig. 4).

ApoA-I Deficiency Does Not Change the Level of Soluble Aβ and Soluble Aβ Oligomers in 12-month-old APP/PS1 Mice—We have shown previously that in APP23 mice with only one copy of endogenous mouse *Abca1* (*Abca1*$^{+/-}$), the level of soluble Aβ oligomers correlated with memory deficits (31). To examine if the memory deficits in APP/PS1/KO used in this study correlate with the levels of soluble Aβ oligomers, we performed dot blotting using anti-oligomeric A11 and OC antibodies. The A11 and OC antibodies are conformation-dependent and were shown to detect prefibrillar and fibrillar Aβ oligomers, respectively (35, 36). Soluble proteins were extracted from the cortices and hippocampi using TBS-based extraction buffer, and dot blotting was performed with A11 and OC antibodies. Staining with 6E10 antibody, which recognizes Aβ monomers and fibrils, was used as a control (not shown). As visible in Fig. 6*A*, there was a trend toward an increase of A11-positive oligomers in APP/PS1/KO mice compared with APP/PS1/WT, but the difference was not significant. Fig. 6*B* demonstrates that there is no difference in OC reactivity between the genotypes. For comparison, we also measured the level of soluble $A\beta_{40}$ and $A\beta_{42}$ using the same extraction. As shown on Fig. 6, in APP/PS1/KO mice compared with APP/PS1/WT, the level of $A\beta_{40}$ was increased (Fig. 6*C*), but $A\beta_{42}$ was unchanged (Fig. 6*D*). The conclusion from these experiments is that the deletion of *Apoa-I* does not change the level of soluble Aβ and Aβ oligomers deposited in the brain.

Lack of ApoA-I Does Not Change Parenchymal Plaque Load and Insoluble Aβ—To determine how the amyloid pathology corresponds to the memory deficits in mice subjected to behavioral testing, the amount of Aβ deposited into plaques was examined using immunohistochemistry. Brain sections were stained with X-34 to visualize fibrillar amyloid plaques. As visible from Fig. 7, *A* and *B*, lack of apoA-I did not affect significantly the level of compact amyloid plaques represented by X-34-positive deposits in the hippocampus and cortex of APP/PS1 mice. Supplemental Fig. 5 demonstrates, in addition, that there was no gender-dependent effect on the plaque load. The level of astrocytosis was determined by glial fibrillary acidic protein staining, and there was no difference between APP/

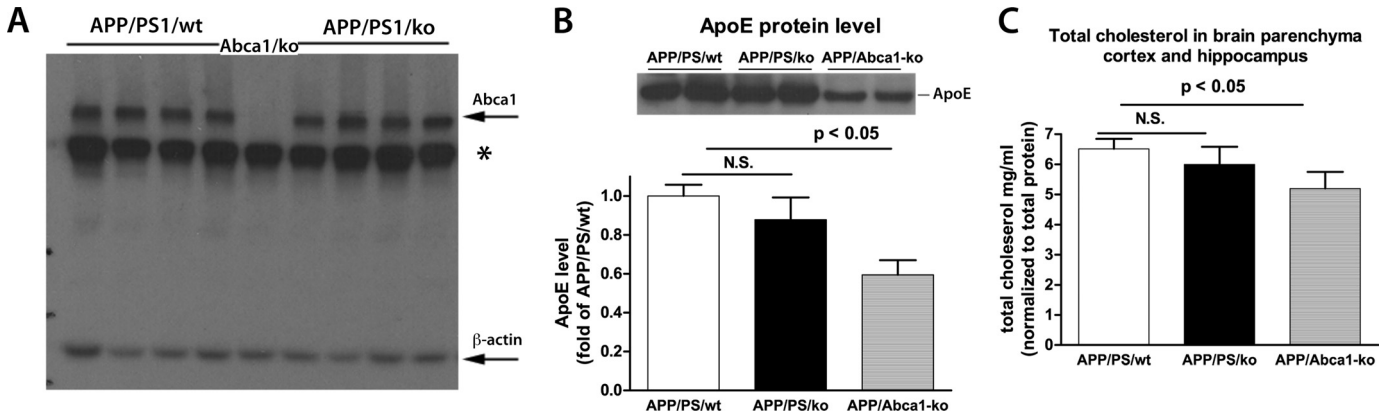

FIGURE 5. **The deletion of apoA-I does not affect protein levels of Abca1 and apoE, and cholesterol concentration in APP/PS1 mice.** *A*, WB for Abca1 was performed on RIPA buffer-extracted brain proteins as described under "Experimental Procedures." *, nonspecific bands. *B*, WB for apoE was performed on TBS-extracted brain proteins. *C*, cholesterol concentration was examined on TBS-extracted brain homogenates using Amplex Red reagent. The values for cholesterol concentration were normalized to the total protein concentration. APP/PS/Abca1^{KO} mice were used as a control. $n = 11$/group. *Error bars*, S.E.

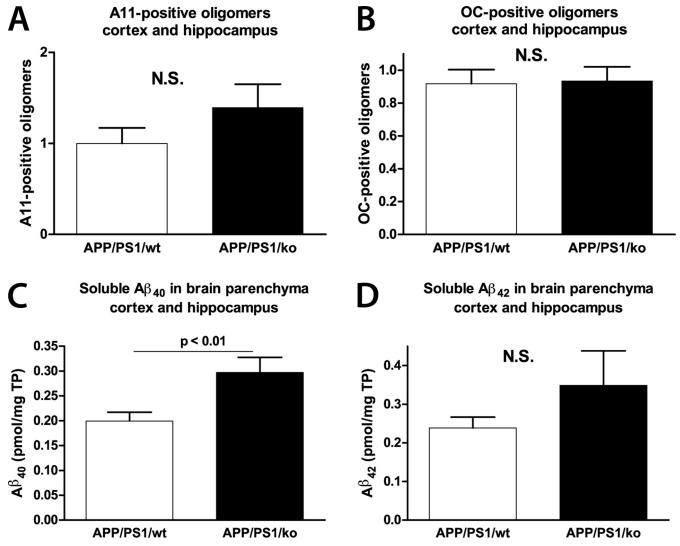

FIGURE 6. **Prefibrillar and fibrillar Aβ oligomers as well as soluble Aβ are not changed by the deletion of apoA-I in APP/PS1 mice.** Soluble proteins were extracted from the cortices and hippocampi of APP/PS1/WT and APP/PS1/KO mice using TBS-based tissue homogenizing buffer as described under "Experimental Procedures." *A*, prefibrillar Aβ oligomers were examined by dot blotting using A11 conformation-specific antibody. *B*, fibrillar Aβ oligomers were examined by dot blotting using OC conformation-specific antibody. In *A* and *B*, dot blot with 6E10 was performed and used to normalize the results of A11 and OC immunoreactivity. Shown is an ELISA for soluble $A\beta_{40}$ (*C*) and $A\beta_{42}$ (*D*). Note that $A\beta_{40}$, unlike $A\beta_{42}$, is significantly increased in APP/PS1/KO mice. Results are from 11–13 mice/group. *Error bars*, S.E.

PS1/WT and APP/PS1/KO mice (supplemental Fig. 6). Next, to confirm the result from X-34 staining, we examined the level of insoluble amyloid, which represents plaque-associated Aβ by ELISA. As shown in Fig. 7, *C* and *D*, there was a gender-dependent increase of insoluble $A\beta_{40}$ and $A\beta_{42}$ in the brains of the female mice inside each genotype. However, we did not find a difference between APP/PS/KO and APP/PS/WT mice. These results clearly demonstrate that the absence of apoA-I does not change the level of compact amyloid plaques in brain parenchyma and insoluble Aβ in the cortex and hippocampus of APP/PS1/KO mice.

ApoA-I Deficiency Increases the Cerebral Amyloid Angiopathy in APP/PS1 Mice—We were puzzled by the lack of obvious difference in amyloid pathology, soluble Aβ oligomers, *Abca1*, or apoE level that could explain the existing memory deficits in APP/PS1/KO. Because in CNS apoA-I is secreted only by the brain microvascular cells (23, 24), we reasoned that its deficiency could affect amyloid deposition in the vicinity of brain blood vessels. To test this, we isolated brain blood vessels from the cortex and hippocampus of 12-month-old APP/PS1/KO and APP/PS1/WT mice and extracted insoluble Aβ using formic acid. As seen in Fig. 8, *A* and *B*, the level of insoluble $A\beta_{40}$ in blood vessels of APP/PS1/KO mice is increased more than 10-fold ($p < 0.05$), and $A\beta_{42}$ is increased by 1.5-fold ($p < 0.05$). The increase of insoluble Aβ was not gender-dependent (supplemental Fig. 7, *A* and *B*). Furthermore, we found that there was a significant negative correlation between memory retention and insoluble $A\beta_{40}$ deposited in the blood vessels (Fig. 8*C*). To determine if apoA-I deficiency affects the evolution of Aβ deposition in the brain blood vessels, we examined mice at 4, 6, and 16 months of age. Our results demonstrate that at an age of 4 months, neither APP/PS1/KO nor APP/PS1/WT had any vascular Aβ. The level of insoluble Aβ in 6-month-old APP/PS1/KO mice, however, was increased in comparison with age-matched APP/PS1/WT ($p < 0.05$; supplemental Fig. 8), whereas the difference between 16-month-old mice of the corresponding genotypes was statistically insignificant. To confirm the results obtained by ELISA, we examined histologically the deposition of amyloid in the vessels of the cortex and hippocampus of 6- and 12-month-old mice. We found that in 6-month-old APP/PS1/WT mice, CAA was very rare, and only two of 10 mice had blood vessels affected by CAA. In contrast, all of the APP/PS1/KO mice had visible CAA, and the difference from APP/PS1/WT was statistically significant (Fig. 8*D*, $p < 0.05$). Fig. 8*D* also demonstrates that in comparison with 12-month-old APP/PS1/WT in age-matched APP/PS1/KO, CAA is increased 1.5-fold (representative images are shown on Fig. 8*E*). Additional processing of the data did not reveal gender dependence (supplemental Fig. 7*C*). Finally, CAA was examined by confocal microscopy using co-staining for fibrillar Aβ and smooth muscle actin. The results of these experiments demonstrated that the vessels affected by CAA are mostly arteries (a representative *image* is shown in Fig. 8*F*). Therefore,

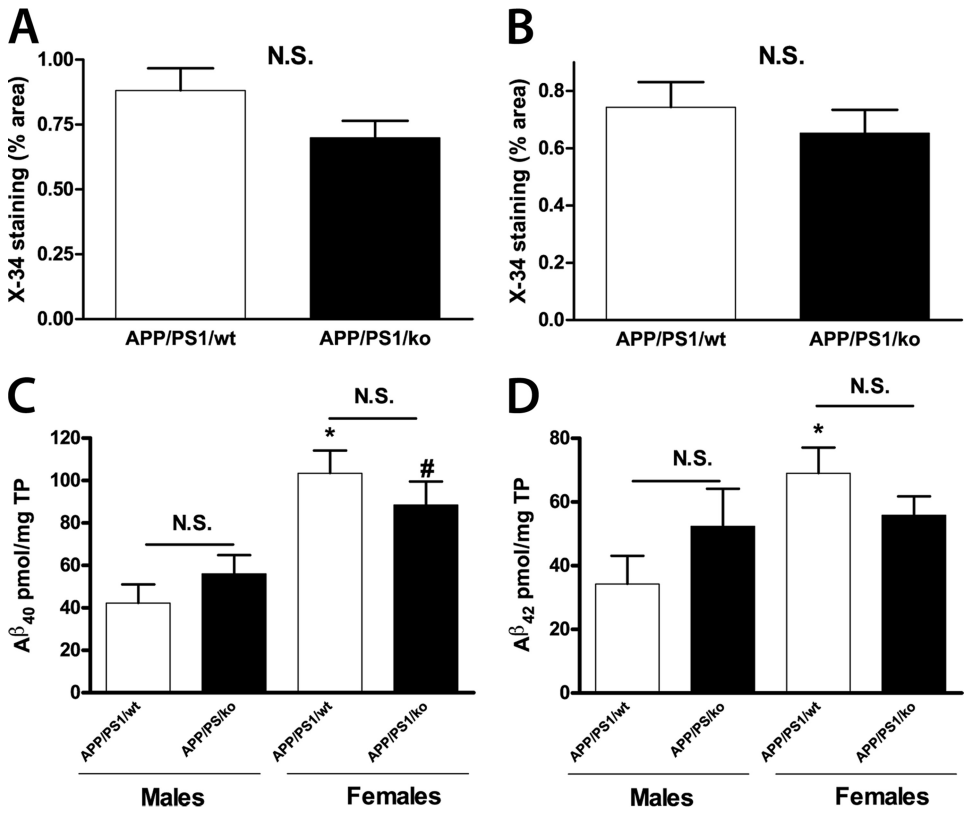

FIGURE 7. **Lack of apoA-I does not affect amyloid plaque load and insoluble Aβ in brain parenchyma of APP/PS1 mice.** *A* and *B*, brain sections were stained with X-34 to visualize fibrillar amyloid plaques from 12-month-old APP/PS1/WT and APP/PS1/KO mice. Shown is a graphical representation of the percentage of area of the hippocampus (*A*) and cortex (*B*) covered by X-34-positive deposits (% *X-34 load*). *C* and *D*, insoluble Aβ was extracted from cortices and hippocampi of 12-month-old APP/PS1/WT and APP/PS1/KO mice using formic acid and $A\beta_{40}$ (*C*) and $A\beta_{42}$ (*D*) determined by ELISA, as explained under "Experimental Procedures." Note that there is an increase in $A\beta_{40}$ and $A\beta_{42}$ in female APP/PS1 mice but no difference between the genotypes (APP/PS1/WT *versus* APP/PS1/KO is not significant (*N.S.*)). *, $p < 0.05$ *versus* male APP/PS/WT; #, $p < 0.05$ *versus* male APP/PS1/KO. Analysis was by Student's *t* test. *Bars*, means ± S.E. For APP/PS1/WT, $n = 7$ males and 6 females; APP/PS1/KO, $n = 6$ males and 5 females. *Error bars*, S.E.

we conclude that the lack of apoA-I in APP/PS1/KO mice increases the build-up of insoluble amyloid in brain blood vessels and affects the age of onset of CAA.

ApoA-I Decreases Apoptotic Cell Death in Primary Human Brain Vascular Smooth Muscle Cells—To determine the mechanism by which Aβ can affect blood vessels and if apoA-I is protective, we used primary vascular smooth muscle cells isolated from human brain (BVSMC). BVSMC were treated with synthetic $A\beta_{40}$ and $A\beta_{42}$ peptides with or without human apoA-I. In these experiments, we also compared the effectiveness of apoA-I lipidation in protecting against Aβ toxicity in BVSMC. In Fig. 9*A*, phase-contrast micrographs demonstrate that when BVSMC were incubated with $A\beta_{42}$ without apoA-I, many cells appear smaller and shrunken, suggesting that they undergo significant damage. In contrast, BVSMC treated with $A\beta_{42}$ plus apoA-I had a flat and healthy appearance. To examine the level of apoptosis, we used a Caspase-Glo 3/7 assay. As shown in Fig. 9, *B* and *C*, non-lipidated apoA-I significantly decreased $A\beta_{40}$- and $A\beta_{42}$-induced apoptosis in BSMVC. We also established that lipidated apoA-I (rHDL) decreased $A\beta_{40}$- and $A\beta_{42}$-induced apoptosis in BVSMC in a similar manner (Fig. 9, *D* and *E*). Therefore, we conclude that apoA-I in lipidated or non-lipidated form is protective against the toxic effects of Aβ in the smooth muscle cells of the vascular wall.

DISCUSSION

Although epidemiological studies have demonstrated that a low level of serum HDL and apoA-I concentrations increase the risk of AD (10, 12, 44), the mechanistic link between HDL/apoA-I and AD is still unknown. In this study we used *in vitro* and *in vivo* model systems to demonstrate that 1) human and mouse apoA-I prevent the formation of high molecular aggregates of $A\beta_{40}$ and $A\beta_{42}$ and decrease Aβ toxicity in primary neurons; 2) the deletion of endogenous *Apoa-I* aggravates the memory deficits in mice expressing mutated human APP and PS1 but not in non-transgenic mice; 3) the deletion of *Apoa-I* increases CAA in APP/PS1 mice and accelerates its appearance, but does not affect parenchymal Aβ deposits; and 4) human apoA-I in lipidated and nonlipidated form is protective against apoptosis caused by Aβ in BVSMC.

The results from *in vitro* experiments with $A\beta_{42}$ presented in this report confirm our previous results with human apoA-I and $A\beta_{40}$ (25). It is noteworthy that the complete inhibition of high molecular aggregates of $A\beta_{42}$ was achieved with equimolar concentrations of apoA-I and $A\beta_{42}$ (Figs. 1 and 2). The effective apoA-I/Aβ ratio used here is lower than their ratio in the CSF and probably in the brain interstitial fluid. For example, the concentration of apoA-I in human CSF is around 4 μg/ml (22), whereas the concentration of $A\beta_{42}$ is 600–700 pg/ml (45), suggesting that in the brain, the interstitium molar ratio of apoA-I and Aβ is probably much higher than the one used in our study. Therefore, the existing conditions *in vivo*, provided that there is no abnormal decrease in apoA-I level, favor the inhibition of $A\beta_{42}$ aggregation by apoA-I. For the *in vitro* experiments in this study, we used lipidated and non-lipidated apoA-I (25–27). Although it is difficult to speculate how apoA-I lipidation affects binding to Aβ, it is obvious that HDL inhibits Aβ aggregation. Therefore, regardless of some differences in binding affinity of apoA-I to Aβ that are possible as a result of apoA-I lipidation, it is clear that either lipid-poor apoA-I or apoA-I, as a component of HDL, exerts an inhibitory effect on Aβ aggregation.

One of the most important findings of the present study is that APP/PS1/KO mice experience substantial cognitive deficits in comparison with APP/PS1/WT mice. It is noteworthy that APP/PS1/KO show significant memory impairment yet without a difference in the levels of parenchymal amyloid load when compared with APP/PS1/WT controls expressing wild

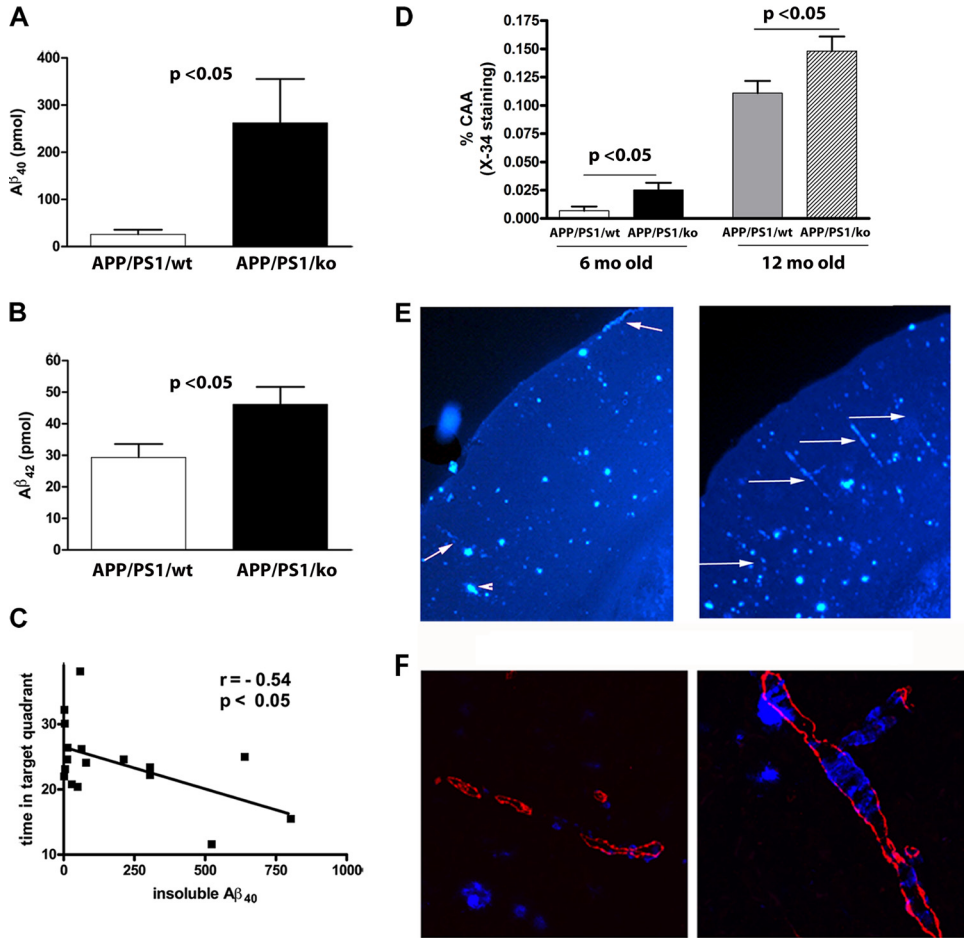

FIGURE 8. **Lack of apoA-I increases CAA in 6- and 12-month-old APP/PS1 mice.** *A* and *B*, blood vessels were isolated from cortices and hippocampi of 12-month-old APP/PS/KO and APP/PS/WT mice, and insoluble Aβ was extracted using formic acid. $A\beta_{40}$ (*A*) and $A\beta_{42}$ (*B*) levels were measured by ELISA as described under "Experimental Procedures." $n = 8–10$ mice/group. *C*, nonparametric analysis demonstrates negative correlation between $A\beta_{40}$ in blood vessels and cognitive performance. Spearman coefficient $r = -0.54$, $p < 0.05$. *D*, CAA is increased in the brains of 6- and 12-month-old mice APP/PS/KO mice as compared with age-matched APP/PS/WT. Amyloid deposits in cerebral blood vessels (cortex and hippocampus) were evaluated using X-34 staining as described under "Experimental Procedures." For 6-month-old mice, $n = 10$; for 12-month-old mice, $n = 13–14$/group. *E*, representative *images* from 12-month-old APP/PS/KO mice and APP/PS/WT mice. The *arrows* point to blood vessels affected by CAA, and *arrowheads* point to the parenchymal deposits. Note that APP/PS/KO mice and APP/PS/WT mice have similar amounts of parenchymal plaques, but APP/PS/KO mice have more CAA. *F*, confocal laser microscope images of CAA in APP/PS/WT and APP/PS/KO mice. Blood vessels are delineated with smooth muscle actin antibody, and compact amyloid plaques are shown with X34 staining. *Error bars*, S.E.

type apoA-I. Moreover, the cognitive deficits could not be linked to the levels of soluble Aβ oligomers, which previously were shown by our group (31) as well as others (46) to correlate with the memory impairment in APP-expressing mice. The absence of changes in AD-like phenotype in terms of Aβ deposits and soluble Aβ in PDAPP/apoA-$I^{-/-}$ mice has been reported in a previous study (28); *Apoa-I* deletion in PDAPP mice caused a significant reduction in total plasma cholesterol, corresponding to a significant reduction in cortical brain cholesterol but with no difference in CSF cholesterol or apoE levels in the periphery and brain. Cognitive performance and the level of vascular amyloid deposits in those mice were not reported. In APP/PS1/KO mice, presented in this report, similarly to PDAPP/apoA-$I^{-/-}$, global disruption of *Apoa-I* does not change the total plaque load or the levels of soluble Aβ. The cognitive performance of APP/PS1/KO animals, however, in comparison with APP/PS1/WT is significantly worse and corresponds to the increase of vascular amyloid deposits. Although the connection between CAA (not only as a morphological sign of AD) and cognitive decline is well established, the question of how the lack of apoA-I in mouse brain results in an increased amount of Aβ vascular deposits remains unanswered. It was reported previously that in humans and mouse models, CAA is favored by a higher $A\beta_{40}/A\beta_{42}$ ratio (47–49). Consistent with those results, our data demonstrate that in 12-month-old *Apoa-I*-deficient mice, there is a much higher increase of $A\beta_{40}$ deposited in the cerebral vessels (10-fold) than $A\beta_{42}$ (1.5-fold). Thus, *Apoa-I* deletion changes the $A\beta_{40}/A\beta_{42}$ ratio from 1:1.3 in APP/PS1/WT mice to 5:1 in APP/PS1/KO mice. There are several possible explanations of this phenomenon. ApoA-I is a major apolipoprotein in the CSF, where its concentration is close to that of apoE and has been unequivocally identified in amyloid plaques. There are at least two sources of the brain apoA-I circulation and secretion by brain microvascular cells (22–24). Therefore, it is possible, that in the brain, the highest concentration of apoA-I is achieved near the blood vessels. Considering the strong inhibitory effect of apoA-I on $A\beta_{42}$ aggregation (demonstrated in this study), we can speculate that a lack of apoA-I facilitates Aβ fibril formation in the vicinity of cerebral blood vessels and increases the deposition of Aβ in the vessel walls. The consequence would be a decreased viability of vascular smooth muscle cells, further affecting the contractility of the brain vessels. Thus, both the increased deposition of Aβ in the vessel wall and the increased death of vascular smooth muscle cells facilitate CAA. Such a possibility does not exclude, however, a direct and still unknown effect of apoA-I on the permeability of BBB for Aβ and its clearance from the brain. Because of the localized morphological changes and indistinguishable total Aβ load between APP/PS1/KO and APP/PS1/WT mice, other mechanisms like inefficient extracellular proteolytic degradation of Aβ by insulin-degrading enzyme or neprilysin or impaired receptor-mediated internalization of different Aβ-protein complexes seem unlikely.

In agreement with our data, a study by Lewis *et al.* (53) found that the transgenic overexpression of human apoA-I

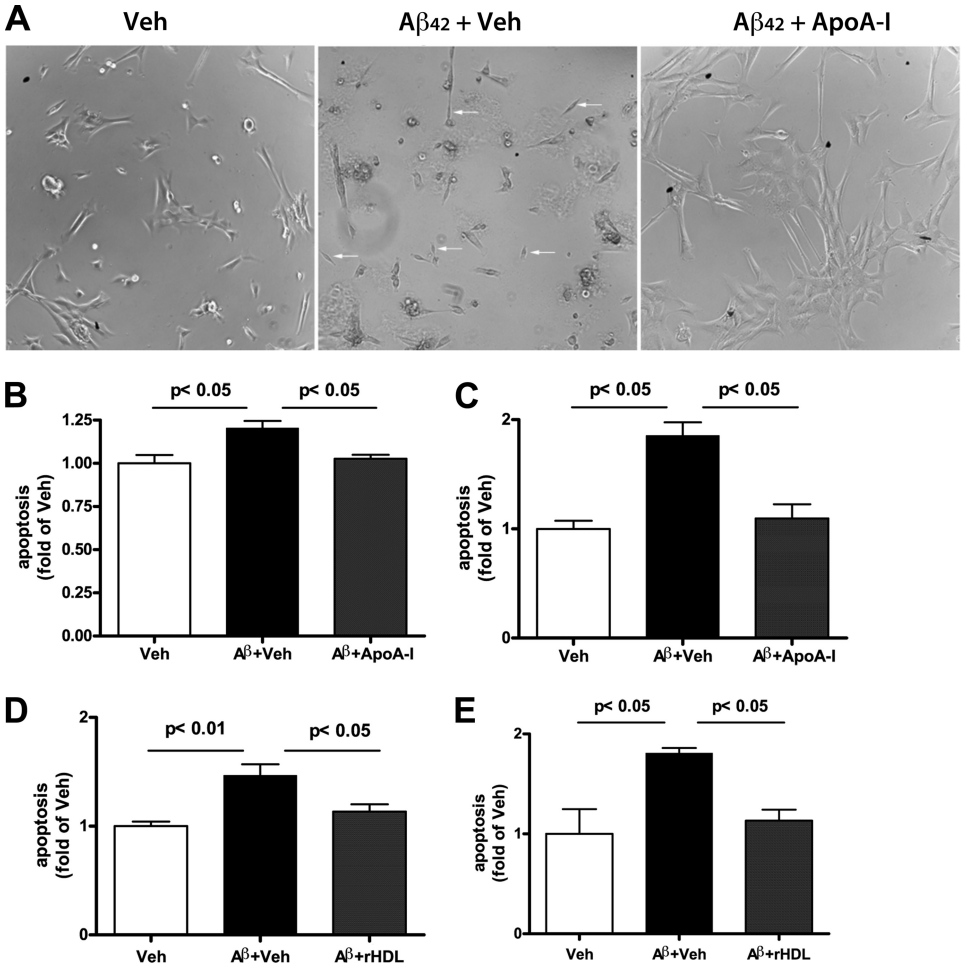

FIGURE 9. **ApoA-I decreases apoptotic cell death in primary BVSMC.** BVSMC were incubated with 3 μM Aβ peptides with or without 3 μM human apoA-I for 24 h, and apoptosis was measured by the Caspase-Glo 3/7 assay. *A*, phase-contrast microphotographs show the morphology of BSMC after treatment with vehicle (*Veh*), Aβ_{42} plus vehicle (*Aβ_{42} + Veh*) and Aβ_{42} plus apoA-I (*Aβ_{42} + ApoA-I*). Non-lipidated human apoA-I was used in this experiment. Note the difference in the appearance of BSMC treated with Aβ_{42} plus Veh and Aβ_{42} plus apoA-I. The *arrow* points to the presence of shrunken cells, which are probably apoptotic. *B* and *C*, BVSMC were treated with Aβ_{40} (*B*) and Aβ_{42} (*C*) with or without non-lipidated human apoA-I. *D* and *E*, BSMC were treated with Aβ_{40} (*D*) and Aβ_{42} (*C*) with or without lipidated human apoA-I (*rHDL*). *Error bars*, S.E.

in APP/PS1ΔE9 ameliorated memory deficits. In their model APP/PS1/A1, consistent with the results of this report, there was no difference in parenchymal Aβ load. The authors explain the improvement of behavior deficits by anti-inflammatory potential of overexpressed human apoA-I.

Altogether, the results of this study are not surprising, and they provide further experimental support to the available epidemiological data, revealing the possible role of apoA-I in the pathogenesis of AD. A number of cross-sectional studies have already identified an association between apoA-I and AD or dementia, and in all case-control reports, apoA-I levels were lower in subjects with dementia compared with controls (10, 12, 50, 51). A prospective study in a population sample of Japanese-American men confirmed the association of lower apoA-I levels with increased dementia risk, whereas men in the highest quartile of apoA-I concentration had a significantly lower risk (44). The results of all of those studies emphasize the importance of sufficient amount and functional apoA-I in the brain for normal cognitive performance, particularly in older individuals.

It has been increasingly recognized that age-dependent progressive cerebrovascular Aβ deposition causes cerebrovascular degeneration paralleled by cognitive decline (52). Although the age-dependent progression of memory deficits in APP/PS1/KO mice was not the main goal of this study, the demonstration of age-dependent increase of vascular amyloid deposition in brains of animals lacking *Apoa-I* provides further mechanistic support to the hypothesis that dysfunctional apoA-I plays an important role in the progression of AD. In humans, conditions of complete absence of apoA-I due to point mutations or deletions are extremely rare. Changes in regulatory mechanisms controlling the amount and functional efficiency of apoA-I, like genetic variation in *ABCA1*, as a primary cause for apoA-I dysfunction in the vicinity of brain microvasculature may well be the explanation of impaired function of apoA-I in the brain and its role in the pathogenesis of AD and cognitive decline. In this respect, the results of this study help to better understand the role of apoA-I in AD and stimulate additional studies in AD animal models to reveal perturbed amyloid clearing mechanisms in cases of dysfunctional apoA-I.

In conclusion, the data presented in this report complement the results from previous and recent experimental (including the report by Lewis *et al.* (53)), epidemiological, and clinical studies suggesting that apoA-I could participate in AD pathogenesis in several ways: 1) by maintaining Aβ soluble and decreasing its aggregation, which facilitates Aβ efflux from the brain; 2) by maintaining conditions for normal cognitive performance; 3) by its antiatherogenic effect with sustainable blood supply to the brain and reduced vascular injury, and 4) by its anti-inflammatory and antioxidative effects.

Acknowledgments—We are grateful to S. Rasool, J. Wu, and Charles Glabe (University of California, Irvine, CA) for providing A11 and OC antioligomeric antibodies; to Dr. M. Phillips (Children's Hospital of Philadelphia, Philadelphia, PA), who generously provided recombinant mouse apoA-I protein; and to Delbert Gillespie (Center for Clinical Pharmacology, University of Pittsburgh, Pittsburgh, PA) for technical help with human BVSMC.

REFERENCES

1. Alonzo, N. C., Hyman, B. T., Rebeck, G. W., and Greenberg, S. M. (1998) *J. Neuropathol. Exp. Neurol.* **57,** 353–359
2. Bates, K. A., Sohrabi, H. R., Rodrigues, M., Beilby, J., Dhaliwal, S. S., Taddei, K., Criddle, A., Wraith, M., Howard, M., Martins, G., Paton, A., Mehta, P., Foster, J. K., Martins, I. J., Lautenschlager, N. T., Mastaglia, F. L., Laws, S. M., Gandy, S. E., and Martins, R. N. (2009) *J. Alzheimers Dis.* **17,** 305–318
3. Bell, R. D., and Zlokovic, B. V. (2009) *Acta Neuropathol.* **118,** 103–113
4. Bieschke, J., Russ, J., Friedrich, R. P., Ehrnhoefer, D. E., Wobst, H., Neugebauer, K., and Wanker, E. E. (2010) *Proc. Natl. Acad. Sci. U.S.A.* **107,** 7710–7715
5. Bonarek, M., Barberger-Gateau, P., Letenneur, L., Deschamps, V., Iron, A., Dubroca, B., and Dartigues, J. F. (2000) *Neuroepidemiology* **19,** 141–148
6. Bouwman, F. H., Schoonenboom, N. S., Verwey, N. A., van Elk, E. J., Kok, A., Blankenstein, M. A., Scheltens, P., and van der Flier, W. M. (2009) *Neurobiol. Aging* **30,** 1895–1901
7. DeMattos, R. B., O'dell, M. A., Parsadanian, M., Taylor, J. W., Harmony, J. A., Bales, K. R., Paul, S. M., Aronow, B. J., and Holtzman, D. M. (2002) *Proc. Natl. Acad. Sci. U.S.A.* **99,** 10843–10848
8. Dietschy, J. M., and Turley, S. D. (2001) *Curr. Opin. Lipidol.* **12,** 105–112
9. Fagan, A. M., Christopher, E., Taylor, J. W., Parsadanian, M., Spinner, M., Watson, M., Fryer, J. D., Wahrle, S., Bales, K. R., Paul, S. M., and Holtzman, D. M. (2004) *Am. J. Pathol.* **165,** 1413–1422
10. Fagan, A. M., Younkin, L. H., Morris, J. C., Fryer, J. D., Cole, T. G., Younkin, S. G., and Holtzman, D. M. (2000) *Ann. Neurol.* **48,** 201–210
11. Fillit, H., Nash, D. T., Rundek, T., and Zuckerman, A. (2008) *Am. J. Geriatr. Pharmacother.* **6,** 100–118
12. Fitz, N. F., Cronican, A., Pham, T., Fogg, A., Fauq, A. H., Chapman, R., Lefterov, I., and Koldamova, R. (2010) *J. Neurosci.* **30,** 6862–6872
13. Fryer, J. D., Simmons, K., Parsadanian, M., Bales, K. R., Paul, S. M., Sullivan, P. M., and Holtzman, D. M. (2005) *J. Neurosci.* **25,** 2803–2810
14. Glabe, C. G. (2008) *J. Biol. Chem.* **283,** 29639–29643
15. Hawkes, C. A., and McLaurin, J. (2009) *Proc. Natl. Acad. Sci. U.S.A.* **106,** 1261–1266
16. Herzig, M. C., Winkler, D. T., Burgermeister, P., Pfeifer, M., Kohler, E., Schmidt, S. D., Danner, S., Abramowski, D., Stürchler-Pierrat, C., Bürki, K., van Duinen, S. G., Maat-Schieman, M. L., Staufenbiel, M., Mathews, P. M., and Jucker, M. (2004) *Nat. Neurosci.* **7,** 954–960
17. Hsu, M. J., Sheu, J. R., Lin, C. H., Shen, M. Y., and Hsu, C. Y. (2010) *Biochim. Biophys. Acta* **1800,** 290–296
18. Jordán, J., Galindo, M. F., and Miller, R. J. (1997) *J. Neurochem.* **68,** 1612–1621
19. Kawano, M., Kawakami, M., Otsuka, M., Yashima, H., Yaginuma, T., and Ueki, A. (1995) *Clin. Chim. Acta* **239,** 209–211
20. Kayed, R., Head, E., Thompson, J. L., McIntire, T. M., Milton, S. C., Cotman, C. W., and Glabe, C. G. (2003) *Science* **300,** 486–489
21. Kivipelto, M., Helkala, E. L., Hänninen, T., Laakso, M. P., Hallikainen, M., Alhainen, K., Soininen, H., Tuomilehto, J., and Nissinen, A. (2001) *Neurology* **56,** 1683–1689
22. Kivipelto, M., Helkala, E. L., Laakso, M. P., Hänninen, T., Hallikainen, M., Alhainen, K., Soininen, H., Tuomilehto, J., and Nissinen, A. (2001) *BMJ* **322,** 1447–1451
23. Kivipelto, M., Laakso, M. P., Tuomilehto, J., Nissinen, A., and Soininen, H. (2002) *CNS Drugs* **16,** 435–444
24. Kivipelto, M., Ngandu, T., Fratiglioni, L., Viitanen, M., Kåreholt, I., Winblad, B., Helkala, E. L., Tuomilehto, J., Soininen, H., and Nissinen, A. (2005) *Arch. Neurol.* **62,** 1556–1560
25. Koldamova, R., Staufenbiel, M., and Lefterov, I. (2005) *J. Biol. Chem.* **280,** 43224–43235
26. Koldamova, R. P., Lefterov, I. M., Ikonomovic, M. D., Skoko, J., Lefterov, P. I., Isanski, B. A., DeKosky, S. T., and Lazo, J. S. (2003) *J. Biol. Chem.* **278,** 13244–13256
27. Koldamova, R. P., Lefterov, I. M., Lefterova, M. I., and Lazo, J. S. (2001) *Biochemistry* **40,** 3553–3560
28. Koldamova, R. P., Lefterov, I. M., Staufenbiel, M., Wolfe, D., Huang, S., Glorioso, J. C., Walter, M., Roth, M. G., and Lazo, J. S. (2005) *J. Biol. Chem.* **280,** 4079–4088
29. Kuo, Y. M., Emmerling, M. R., Bisgaier, C. L., Essenburg, A. D., Lampert, H. C., Drumm, D., and Roher, A. E. (1998) *Biochem. Biophys. Res. Commun.* **252,** 711–715
30. Kuriyama, M., Takahashi, K., Yamano, T., Hokezu, Y., Togo, S., Osame, M., and Igakura, T. (1994) *Jpn. J. Psychiatry Neurol.* **48,** 589–593
31. LaDu, M. J., Lukens, J. R., Reardon, C. A., and Getz, G. S. (1997) *J. Neurosci. Res.* **49,** 9–18
32. Lefterov, I., Bookout, A., Wang, Z., Staufenbiel, M., Mangelsdorf, D., and Koldamova, R. (2007) *Mol. Neurodegener.* **2,** 20
33. Lefterov, I., Fitz, N. F., Cronican, A., Lefterov, P., Staufenbiel, M., and Koldamova, R. (2009) *ASN Neuro.* **1,** 65–76
34. Lesser, G., Kandiah, K., Libow, L. S., Likourezos, A., Breuer, B., Marin, D., Mohs, R., Haroutunian, V., and Neufeld, R. (2001) *Dement. Geriatr. Cogn. Disord.* **12,** 138–145
35. Linsel-Nitschke, P., and Tall, A. R. (2005) *Nat. Rev. Drug Discov.* **4,** 193–205
36. Maezawa, I., Jin, L. W., Woltjer, R. L., Maeda, N., Martin, G. M., Montine, T. J., and Montine, K. S. (2004) *J. Neurochem.* **91,** 1312–1321
37. Matsubara, E., Soto, C., Governale, S., Frangione, B., and Ghiso, J. (1996) *Biochem. J.* **316,** 671–679
38. Merched, A., Xia, Y., Visvikis, S., Serot, J. M., and Siest, G. (2000) *Neurobiol. Aging* **21,** 27–30
39. O'Nuallain, B., Thakur, A. K., Williams, A. D., Bhattacharyya, A. M., Chen, S., Thiagarajan, G., and Wetzel, R. (2006) *Methods Enzymol.* **413,** 34–74
40. Panzenboeck, U., Balazs, Z., Sovic, A., Hrzenjak, A., Levak-Frank, S., Wintersperger, A., Malle, E., and Sattler, W. (2002) *J. Biol. Chem.* **277,** 42781–42789
41. Paula-Lima, A. C., Tricerri, M. A., Brito-Moreira, J., Bomfim, T. R., Oliveira, F. F., Magdesian, M. H., Grinberg, L. T., Panizzutti, R., and Ferreira, S. T. (2009) *Int. J. Biochem. Cell Biol.* **41,** 1361–1370
42. Pitas, R. E., Boyles, J. K., Lee, S. H., Hui, D., and Weisgraber, K. H. (1987) *J. Biol. Chem.* **262,** 14352–14360
43. Saczynski, J. S., White, L., Peila, R. L., Rodriguez, B. L., and Launer, L. J. (2007) *Am. J. Epidemiol.* **165,** 985–992
44. Selkoe, D. J. (2008) *Behav. Brain Res.* **192,** 106–113
45. Strittmatter, W. J., Weisgraber, K. H., Huang, D. Y., Dong, L. M., Salvesen, G. S., Pericak-Vance, M., Schmechel, D., Saunders, A. M., Goldgaber, D., and Roses, A. D. (1993) *Proc. Natl. Acad. Sci. U.S.A.* **90,** 8098–8102
46. Tanaka, M., Koyama, M., Dhanasekaran, P., Nguyen, D., Nickel, M., Lund-Katz, S., Saito, H., and Phillips, M. C. (2008) *Biochemistry* **47,** 2172–2180
47. Wahrle, S. E., Jiang, H., Parsadanian, M., Legleiter, J., Han, X., Fryer, J. D., Kowalewski, T., and Holtzman, D. M. (2004) *J. Biol. Chem.* **279,** 40987–40993
48. Weiler-Güttler, H., Sommerfeldt, M., Papandrikopoulou, A., Mischek, U., Bonitz, D., Frey, A., Grupe, M., Scheerer, J., and Gassen, H. G. (1990) *J. Neurochem.* **54,** 444–450
49. Weller, R. O., Boche, D., and Nicoll, J. A. (2009) *Acta Neuropathol.* **118,** 87–102
50. Wilcock, D. M., Gordon, M. N., and Morgan, D. (2006) *Nat. Protoc.* **1,** 1591–1595
51. Wu, J. W., Breydo, L., Isas, J. M., Lee, J., Kuznetsov, Y. G., Langen, R., and Glabe, C. (2010) *J. Biol. Chem.* **285,** 6071–6079
52. Yvan-Charvet, L., Wang, N., and Tall, A. R. (2010) *Arterioscler. Thromb. Vasc. Biol.* **30,** 139–143
53. Lewis, T. L., Cao, D., Lu, H., Mans, R. A., Su, Y. R., Jungbauer, L., Linton, M. F., Fazio, S., LaDu, M. J., and Li, L. (2010) *J. Biol. Chem.* **285,** 36958–36968